Available online at www.sciencedirect.com
ScienceDirect
International Journal of Heat and Mass Transfer 50 (2007) 4446–4456
International Journal of HEAT and MASS TRANSFER
www.elsevier.com/locate/ijhmt

Comparison of the CHF data for water and refrigerant HFC-134a by using the fluid-to-fluid modeling methods

Se-Young Chun [a,*], Sung-Deok Hong [a], Yeon-Sik Cho [b], Won-Pil Baek [a]

[a] *Thermal Hydraulic Safety Research Division, Korea Atomic Energy Research Institute, 150 Dukjin-dong, Yuseong-gu, Daejeon 305-353, South Korea*

[b] *Department of Nuclear R&D Program, Korea Science and Engineering Foundation, 180-1 Gajeong-dong, Yuseong-gu, Daejeon 305-350, South Korea*

Received 11 January 2005
Available online 1 June 2007

Abstract

CHF experiments in tubes and annulus cooled with HFC-134a have been performed. The HFC-134a and water CHF data have been compared by applying the Ahmad and the Katto modeling parameters. For the mass fluxes from 710 to 3500 kg m^{-2} s^{-1} in the tubes, the HFC-134a and water CHF data fall close to the same curve on the plane of the dimensionless CHF vs. the Ahmad and the Katto modeling parameters. For the mass fluxes below 600 kg m^{-2} s^{-1} in an annulus, the dimensionless CHFs as a function of the Ahmad and the Katto modeling parameters show a large difference between the HFC-134a and the water. The Katto and the Ahmad modeling parameters cannot be correlated with the dimensionless CHF data for HFC-134a and water on the same curve in the low mass flux and high quality conditions.

Keywords: Critical heat flux; Tubes; Annulus; HFC-134a; Fluid-to-fluid modeling; Low flow rate

1. Introduction

Most of the critical heat flux (CHF) experiments have been carried out using water as a working fluid because the CHF in water cooled nuclear reactors is one of the important thermal-hydraulic parameters limiting the available power. However, it is not easy for many heat transfer laboratories to carry out the water CHF experiments under the thermal-hydraulic conditions of nuclear reactors, i.e., high pressures and high temperatures. Especially, the CHF experiments for complex geometries such as nuclear fuel bundles require large amounts of electrical power and a large scale facility. In order to reduce the cost and technical difficulties of the water experiments, Freon fluids such as CFC-11, -12, HCFC-22, etc. have been frequently used as working fluids because of their lower latent heat of vaporization and lower critical pressure when compared with water. For a practical application to the nuclear industry, the CHF data from the Freon experiments should be converted into water-equivalent data with a fluid-to-fluid modeling technique.

* Corresponding author. Tel.: +82 42 868 2948; fax: +82 42 868 8362.
E-mail address: sychun@kaeri.re.kr (S.-Y. Chun).

0017-9310/$ - see front matter © 2005 Elsevier Ltd. All rights reserved.
doi:10.1016/j.ijheatmasstransfer.2005.06.039

Nomenclature

C_i	constants in Eq. (13)
D	tube inner diameter (m)
D_h	hydraulic equivalent diameter (m)
G	mass flux (kg m^{-2} s^{-1})
h_{fg}	latent heat of vaporization (kJ kg^{-1})
Δh_{in}	inlet subcooling (kJ kg^{-1})
L	heated length (m)
P	system pressure (MPa)
x	thermodynamic equilibrium quality (−)
x_{CHF}	critical quality (−)
z	distance from the bottom end of the heated section (m)

Greek symbols

ρ	density (kg m^{-3})
σ	surface tension (N m^{-1})
Φ_{CHF}	critical heat flux (kW m^{-2})
ψ_{CHF}	critical heat flux modeling parameter for mass flux (−)

Subscripts

Ahmad	Ahmad's modeling parameter
F	Freon fluid (HFC-134a)
Katto	Katto's modeling parameter
l	liquid phase
v	vapor phase
W	water

Fluid-to-fluid modeling studies have been performed by many researchers in order to predict the CHFs in water from the data obtained with Freon fluids, since the 1960s. An excellent review of previous studies was reported by Doerffer et al. [1]. In recent years, most of the fluid-to-fluid modeling studies have been performed in Canadian research institutes [2–5]. In the fluid-to-fluid modeling, the geometric, thermodynamic and hydrodynamic similarities should be satisfied for both fluids. In addition to these basic similarities, a modeling parameter for the mass flux was introduced in previous studies in order to simulate the mass flux conditions of both systems. It can be expressed in different forms, depending on the investigators [6–8]. Among the fluid-to-fluid modeling methods reported until now, that of Ahmad [7] is most widely accepted. He found seven important dimensionless groups for CHF modeling, which can be divided into the controllable groups and the uncontrollable groups in the CHF experiments, by applying the Buckingham Pi theorem to the dimensional analysis. And then he developed a CHF modeling parameter for the mass flux by employing the compensated distortion technique for the uncontrollable dimensionless groups. Groeneveld et al. [8], for the mass flux modeling parameter, recommended a dimensionless parameter with the mass flux that is used in the generalized CHF correlation developed by Katto [9].

Unfortunately, it is known that the release of Freon fluids to the atmosphere causes an environmental problem because the CFC and HCFC families deplete the ozone layer. Therefore, CFC-11 and -12 were recently replaced with new fluids such as HCFC-123 and HFC-134a, respectively. HCFC-22 and -123, which also have a very low ozone depletion potential, will be replaced with some other fluids in the future. Recently, the experimental studies on a CHF in vertical tubes cooled with HFC-134a have been performed to examine the suitability of the CFC alternatives [2] and to compare the HFC-134a CHF data with the CHF look-up table [10] for water [4]. However, the previous studies on a fluid-to-fluid modeling have been performed mainly for tubes and they did not cover low flow conditions. Moreover, the HFC-134a CHF data has never been compared directly with the water data to assess the performance and distortion of the fluid-to-fluid modeling techniques. The authors have conducted CHF experiments using HFC-134a as a working fluid. CHF experiments for heated round tubes and an internally heated annulus have recently been completed. In this paper, the HFC-134a and water CHF data are compared by applying the existing fluid-to-fluid modeling techniques and an applicable range of the modeling techniques is discussed.

2. HFC-134a CHF experiments

2.1. Experimental loop

The experimental works have been performed in the Freon Thermal-Hydraulic Experimental Loop at the Korea Atomic Energy Research Institute (KAERI). This loop uses HFC-134a as a working fluid and can be operated at pressures of 0.57–4.50 MPa (water equivalent pressures: 3.65–24.49 MPa) and a maximum fluid temperature of 423 K.

Fig. 1 shows the simplified flow diagram of the Freon loop. It basically consists of a main circulating pump, preheater, pressurizer, test section, vapor/liquid separator, condenser and cooler. HFC-134a fluid is circulated in the main loop by a canned motor centrifugal pump.

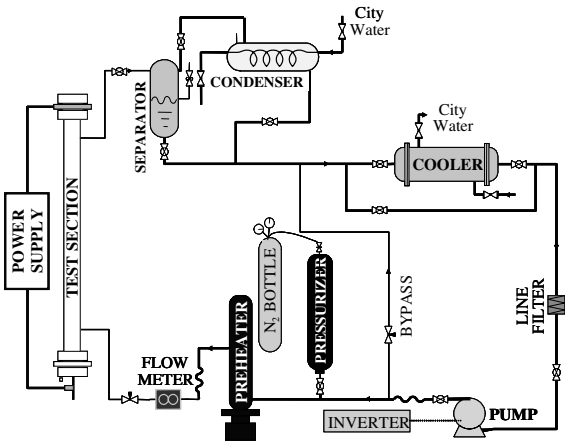

Fig. 1. Schematic diagram of the Freon thermal-hydraulic experimental loop.

The flow rate of the test section inlet is controlled by adjustments of the motor speed of the circulating pump, the flow control valve and the bypass valve. The flow rate of the fluid entering the test section is measured by the Coriolis type mass flow meter. A throttling valve located up stream of the test section inlet is used to avoid a flow fluctuation, which is frequently observed under low flow conditions. The preheater adjusts the degree of subcooling of the fluid entering the test section. In the separator, the vapor phase is separated from the vapor/liquid two-phase mixture generated in the test section. The separated vapor is condensed through the condenser attached to the separator. The accumulator is used as a pressurizer. The system pressure is increased by pressurizing the accumulator using the nitrogen gas pressure and decreased by releasing the nitrogen gas through the release valve connected to the top nozzle of the accumulator. The power applied to the test section is supplied from a 70 V × 1000 A, DC source. Protection for the heater rod of the test section against an excessive temperature is provided by an automatic power run down/trip system, which is operated by the CHF detection and protection system.

2.2. Test sections

In the present study, the CHF data for a uniform axial heat flux distribution and a vertical upward flow from two series of the experiments are used for comparing the water CHF data: (a) round tubes and (b) an internally heated annulus.

Two test section tubes, which are made of Inconel 600 with 9.40 and 7.75 mm inner diameters, were used in the tube experiments. A sketch of the test section is shown in Fig. 2. The test sections are heated directly by means of a large DC current passing through the wall and the heated length is changed from 0.6 to 2.6 m by moving the lower power clamp. For detecting a CHF occurrence, three T-type ungrounded thermocouples with a sheath outer diameter of 0.5 mm are fixed to the outer wall surface of the tube by wooden clips. The temperature sensing points are located at 10, 15 and 20 mm from the top end of the heated section.

In the annulus experiments, in order to simplify the comparison between the HFC-134a and water CHF data by applying the fluid-to-fluid modeling techniques, the test section has the same geometry as the annulus test section in the water CHF experiments which the authors performed in previous studies [11,12]. Fig. 2 shows the details of the test section used in the annulus experiments. The test section consists of an outer pipe with a 19.4 mm inside diameter and an inner heater rod with a 9.54 mm outer diameter having a heated length of 1842 mm. The heater rod is heated directly by a large DC current and the heated section is made of Inconel 601 tube. For detecting the CHF occurrence, two K-type ungrounded thermocouples with a sheath outer diameter of 0.5 mm are attached to the inside wall surface of the heater rod. The temperature sensing points are located at 10 and 30 mm from the top end of the heated section.

2.3. Experimental procedure and conditions

The CHF experiments have been performed using the following procedure. First, the flow rate, inlet subcooling and system pressure (at the test section outlet) are set to the desired levels. Power is then applied to the heated section of the test section and increased gradually in small steps while the test section inlet conditions are maintained at constant values. CHF conditions are defined as a sharp and continuous rise of the wall temperatures of the heated section. The CHF detection and protection system continuously scans the temperature signals from the thermocouples attached to the heated wall. When the wall temperature reaches a pre-determined set point, the DC power to the heated section is automatically decreased or tripped by the power run down/trip system. The experimental conditions under which the CHF data have been obtained are as follows:

(a) Tube experiments
- system pressure: 1.5–2.9 MPa (water equivalent pressure: 9.2–16.7 MPa),
- mass flux: 710–3500 kg m^{-2} s^{-1},
- inlet subcooling: 11–70 kJ kg^{-1},
- critical quality: −0.20–0.48.

(b) Annulus experiments
- system pressure: 1.0–2.7 MPa (water equivalent pressure: 6.3–15.5 MPa),

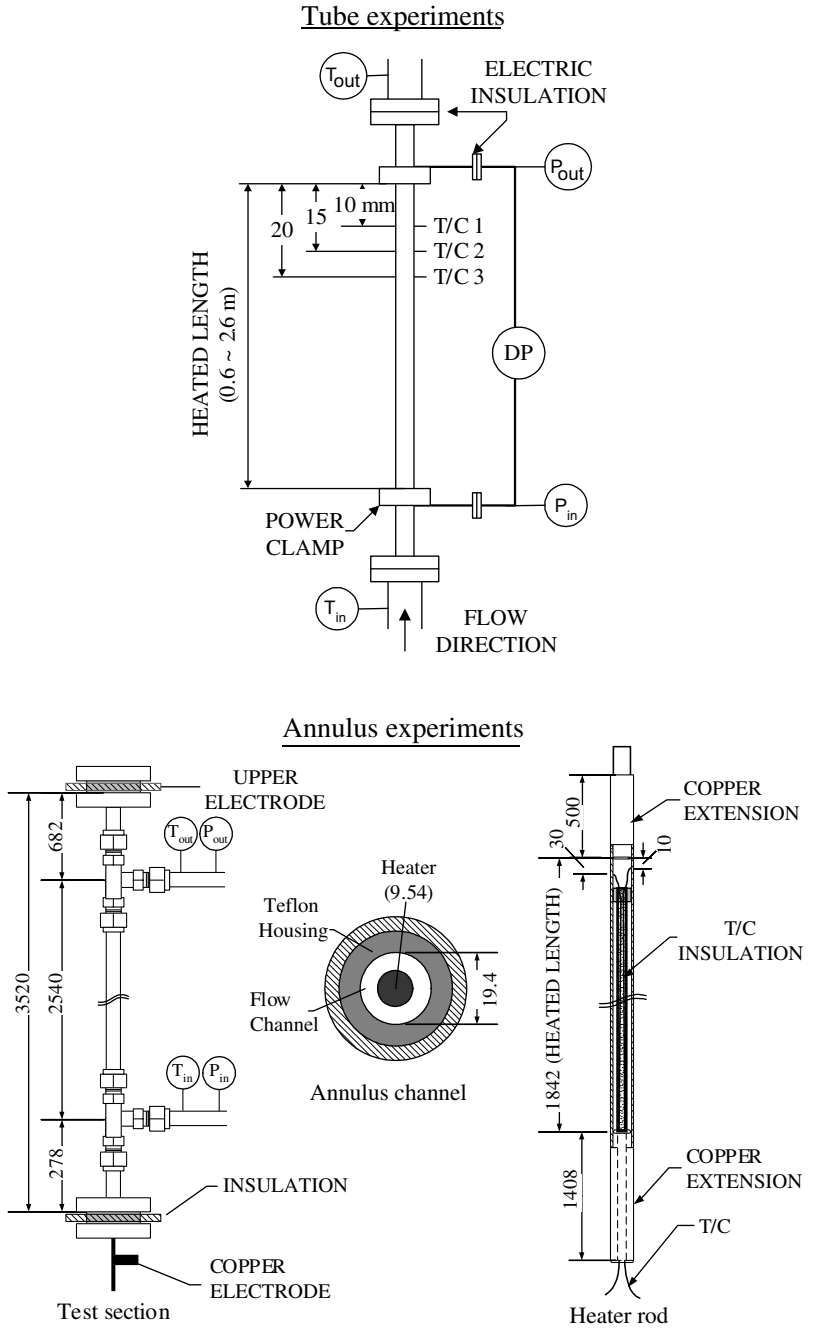

Fig. 2. Test sections.

- mass flux: 150–1140 kg m^{-2} s^{-1},
- inlet subcooling: 12–38 kJ kg^{-1},
- critical quality: 0.00–0.70.

The pressure at the outlet of the test section is specified as the system pressure. The water equivalent pressures are determined from the density ratio of the liquid to the vapor. The critical quality is the thermodynamic quality at a CHF location calculated from the heat balance of the test section. The main parameters measured in the present experiments are the fluid temperatures at the inlet and outlet of the test section, the wall temperatures of the heated section, the pressures at the inlet and outlet of the test section, the flow rate

and the power applied to the heated section. For the performance of the experiments and analysis of the experimental data, the thermodynamic properties of HFC-134a from NIST REFPROP version 6.01 [13] are used. The uncertainties of the measuring system are estimated from a calibration of the sensors and the accuracy of the equipment, according to a propagation error analysis based on Taylor's series method [14]. The evaluated maximum uncertainties of the pressures, flow rates and temperatures are less than ±0.3%, ±0.3% and ±0.7 K of the readings in the range of interest, respectively. The uncertainty of the heat flux calculated from the applied power is always less than ±1.8% of the readings. The heat loss in the test section should be taken into account in the calculation of the heat flux. Before starting a set of experiments, pretests (i.e., heat balance tests) were carried out to estimate the heat loss in the test section. The heat losses estimated by the pretests for each pressure condition is less than 1.0% of the power input.

3. Fluid-to-fluid modeling technique

Generally, a fluid-to-fluid modeling requires three basic similarities, which can be easily achieved experimentally.

Geometric similarity: $$\left(\frac{L}{D}\right)_{\mathrm{W}} = \left(\frac{L}{D}\right)_{\mathrm{F}}, \tag{1}$$

Thermodynamic similarity: $$\left(\frac{\Delta h_{\mathrm{in}}}{h_{\mathrm{fg}}}\right)_{\mathrm{W}} = \left(\frac{\Delta h_{\mathrm{in}}}{h_{\mathrm{fg}}}\right)_{\mathrm{F}} \tag{2}$$

Hydrodynamic similarity: $$\left(\frac{\rho_{\mathrm{l}}}{\rho_{\mathrm{v}}}\right)_{\mathrm{W}} = \left(\frac{\rho_{\mathrm{l}}}{\rho_{\mathrm{v}}}\right)_{\mathrm{F}}, \tag{3}$$

where subscript 'W' denotes the equivalent value for water and subscript 'F' indicates the Freon fluid. The symbols are defined in the nomenclature. In addition to the above basic similarities, a mass flux similarity is needed, i.e., the fluid-to-fluid modeling also requires the same dimensionless mass flux for both fluids as an additional hydrodynamic similarity. Therefore, the dimensionless parameter based on the Reynolds number GD/μ_{l} should be included in the above similarities.

Ahmad [7] chose seven important dimensionless groups for CHF by applying Buckingham's Pi theorem to the dimensional analysis, and then by employing the compensated distortion technique, the dimensionless equation was expressed as

$$\frac{\Phi_{\mathrm{CHF}}}{Gh_{\mathrm{fg}}} = f\left(\psi_{\mathrm{CHF-Ahmad}}, \frac{\Delta h_{\mathrm{in}}}{h_{\mathrm{fg}}}, \frac{\rho_{\mathrm{l}}}{\rho_{\mathrm{v}}}, \frac{L}{D}\right), \tag{4}$$

where $\psi_{\mathrm{CHF\text{-}Ahmad}}$ can be presumed to be the modeling parameter for a dimensionless mass flux

$$\psi_{\mathrm{CHF-Ahmad}} = \left(\frac{GD}{\mu_{\mathrm{l}}}\right)\left(\frac{\mu_{\mathrm{l}}}{\sqrt{\sigma D\rho_{\mathrm{l}}}}\right)^{2/3}\left(\frac{\mu_{\mathrm{l}}}{\mu_{\mathrm{v}}}\right)^{1/5}. \tag{5}$$

If Eqs. (1)–(3) and $(\psi_{\mathrm{CHF}})_{\mathrm{W}} = (\psi_{\mathrm{CHF}})_{\mathrm{F}}$ are satisfied, then the dimensionless CHF (i.e., boiling number) of the left hand side of Eq. (4) should be the same for both fluids.

$$\left(\frac{\Phi_{\mathrm{CHF}}}{Gh_{\mathrm{fg}}}\right)_{\mathrm{W}} = \left(\frac{\Phi_{\mathrm{CHF}}}{Gh_{\mathrm{fg}}}\right)_{\mathrm{F}}. \tag{6}$$

Ahmad showed that $\Phi_{\mathrm{CHF}}/Gh_{\mathrm{fg}}$ vs. ψ_{CHF} for different fluids fall on the same curve for fixed $\Delta h_{\mathrm{in}}/h_{\mathrm{fg}}$, $\rho_{\mathrm{l}}/\rho_{\mathrm{v}}$ and L/D.

A generalized correlation of CHF for flow boiling in a vertical tube developed by Katto [9] is expressed by the following dimensionless groups:

$$\frac{\Phi_{\mathrm{CHF}}}{Gh_{\mathrm{fg}}} = f\left(\frac{GD}{\mu_{\mathrm{l}}}, \frac{\Delta h_{\mathrm{in}}}{h_{\mathrm{fg}}}, \frac{\rho_{\mathrm{l}}}{\rho_{\mathrm{v}}}, \frac{L}{D}, \frac{\mu_{\mathrm{l}}}{\sqrt{\sigma D\rho_{\mathrm{l}}}}\right).$$

This equation can be rewritten as follows:

$$\frac{\Phi_{\mathrm{CHF}}}{Gh_{\mathrm{fg}}} = f\left(\frac{G\sqrt{D}}{\sqrt{\sigma\rho_{\mathrm{l}}}}, \frac{\Delta h_{\mathrm{in}}}{h_{\mathrm{fg}}}, \frac{\rho_{\mathrm{l}}}{\rho_{\mathrm{v}}}, \frac{L}{D}\right). \tag{7}$$

Groeneveld et al. [8] recommended the dimensionless group $G(D/\sigma\rho_{\mathrm{l}})^{1/2}$ as the modeling parameter ψ_{CHF} for the fluid-to-fluid modeling because of its simpler form.

$$\psi_{\mathrm{CHF-Katto}} = \frac{G\sqrt{D}}{\sqrt{\sigma\rho_{\mathrm{l}}}}. \tag{8}$$

Once all the similarities including the modeling parameter for a dimensionless mass flux are achieved, the water CHF can be calculated by Eq. (6).

$$(\Phi_{\mathrm{CHF}})_{\mathrm{W}} = \left(\frac{\Phi_{\mathrm{CHF}}}{Gh_{\mathrm{fg}}}\right)_{\mathrm{F}}(Gh_{\mathrm{fg}})_{\mathrm{W}}. \tag{9}$$

The thermodynamic similarity of Eq. (2) is based on the inlet conditions in the heated section. On the other hand, from the viewpoint of the local conditions, the thermodynamic similarity can be achieved when the thermodynamic qualities in both systems are equal to each other at any axial location z/D along the heated length, i.e.,

$$(x(z))_{\mathrm{W}} = (x(z))_{\mathrm{F}}. \tag{10}$$

For a uniformly heated tube, the critical quality x_{CHF} is given by the following heat balance equation:

$$x_{\mathrm{CHF}} = 4\left(\frac{\Phi_{\mathrm{CHF}}}{Gh_{\mathrm{fg}}}\right)\left(\frac{L}{D}\right) - \left(\frac{\Delta h_{\mathrm{in}}}{h_{\mathrm{fg}}}\right). \tag{11}$$

In this case, Eqs. (4) and (7) based on the inlet conditions are rewritten as follows:

$$\frac{\Phi_{\mathrm{CHF}}}{Gh_{\mathrm{fg}}} = f\left(\psi_{\mathrm{CHF}}, x_{\mathrm{CHF}}, \frac{\rho_{\mathrm{l}}}{\rho_{\mathrm{v}}}, \frac{L}{D}\right). \tag{12}$$

When Eq. (12) based on the local conditions is used, the heat balance in the heated section, i.e., Eq. (11) should be satisfied.

4. Comparison of the CHF data for HFC-134a and water

It is all but impossible to select the CHF data sets of water and Freon that perfectly satisfy the basic similarities of Eqs. (1)–(3) and the same conditions for the modeling parameters from among the CHF data obtained from independent experiments. In addition, the applicability of Ahmad's and Katto's modeling parameters for the mass flux of Eqs. (5) and (8) have not been confirmed for a wide range of flow parameters as yet [4,5]. Therefore, in the present study, the CHF values for HFC-134a cannot be compared directly with those for water. The water CHF data has been processed as it can be compared with the HFC-134a CHF data, and the dimensionless CHF Φ_{CHF}/Gh_{fg} as a function of the modeling parameter for the mass flux ψ_{CHF} is compared for water and HFC-134a.

4.1. Tubes

First, some characteristics of the HFC-134a CHF data obtained from the present experiments are shown in Figs. 3–5. In Figs. 3 and 4, the CHFs are plotted as a function of the pressure. For a mass flux of 710 kg m^{-2} s^{-1}, the CHF decreases monotonously as the pressure increases, and the CHFs for a high mass flux of 3500 kg m^{-2} s^{-1} and the heated length of 1.2 and 2.0 m maintain a nearly constant value with the increasing pressure. Fig. 4 represents a common feature of the effect of the pressure on the present CHF data. For a fixed heated length, tube inner diameter and inlet subcooling, the slope of the decreasing CHF with the pressure becomes gradually steep as the mass flux decreases. The comparison between the CHFs for the tube inner diameters of 7.75 and 9.40 mm is made in Fig. 5, which shows the CHF as a function of the mass flux with the heated length as a parameter. In the case of the heated lengths of 0.6 and 1.2 m, the difference between the CHF values for the tube inner diameters of 7.75 and 9.40 mm is large at a high mass flux of 3500 kg m^{-2} s^{-1}. This difference in the CHF values becomes gradually smaller as the mass flux decreases, and almost disappears at a mass flux of 710 kg m^{-2} s^{-1}. The behavior of the CHF with a mass flux for the heated length of 2.0 m shows that the effect of the tube inner diameter on a CHF scarcely depends on the variations in the mass flux.

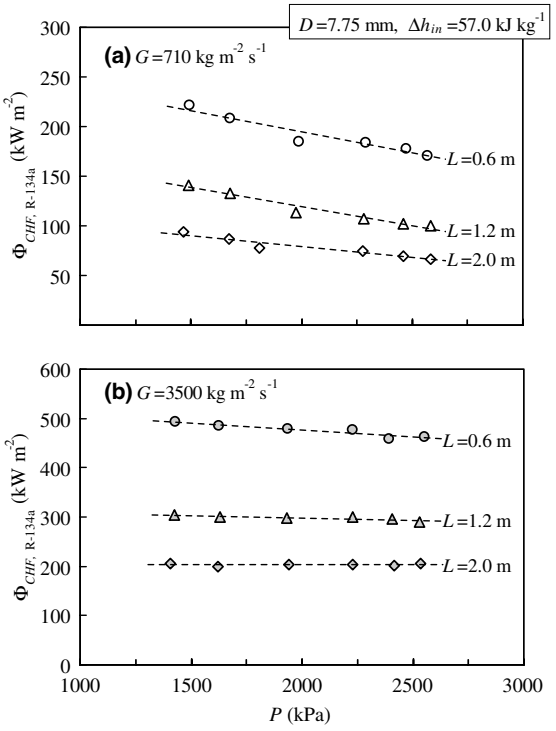

Fig. 3. Effect of the pressure on a HFC-134a CHF.

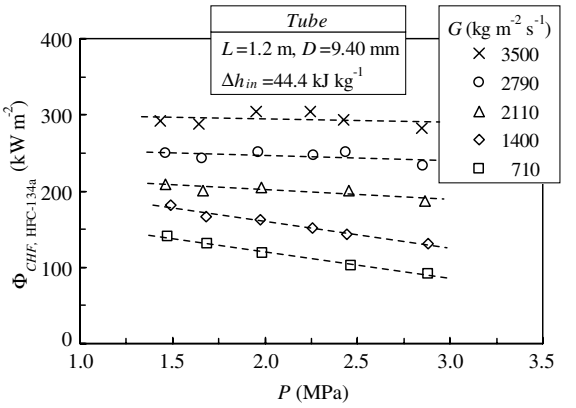

Fig. 4. HFC-134a CHF as a function of the pressure with the mass flux as a parameter.

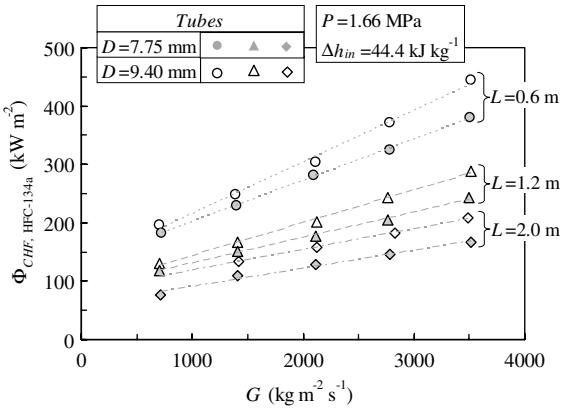

Fig. 5. Effect of the tube inner diameter on a HFC-134a CHF.

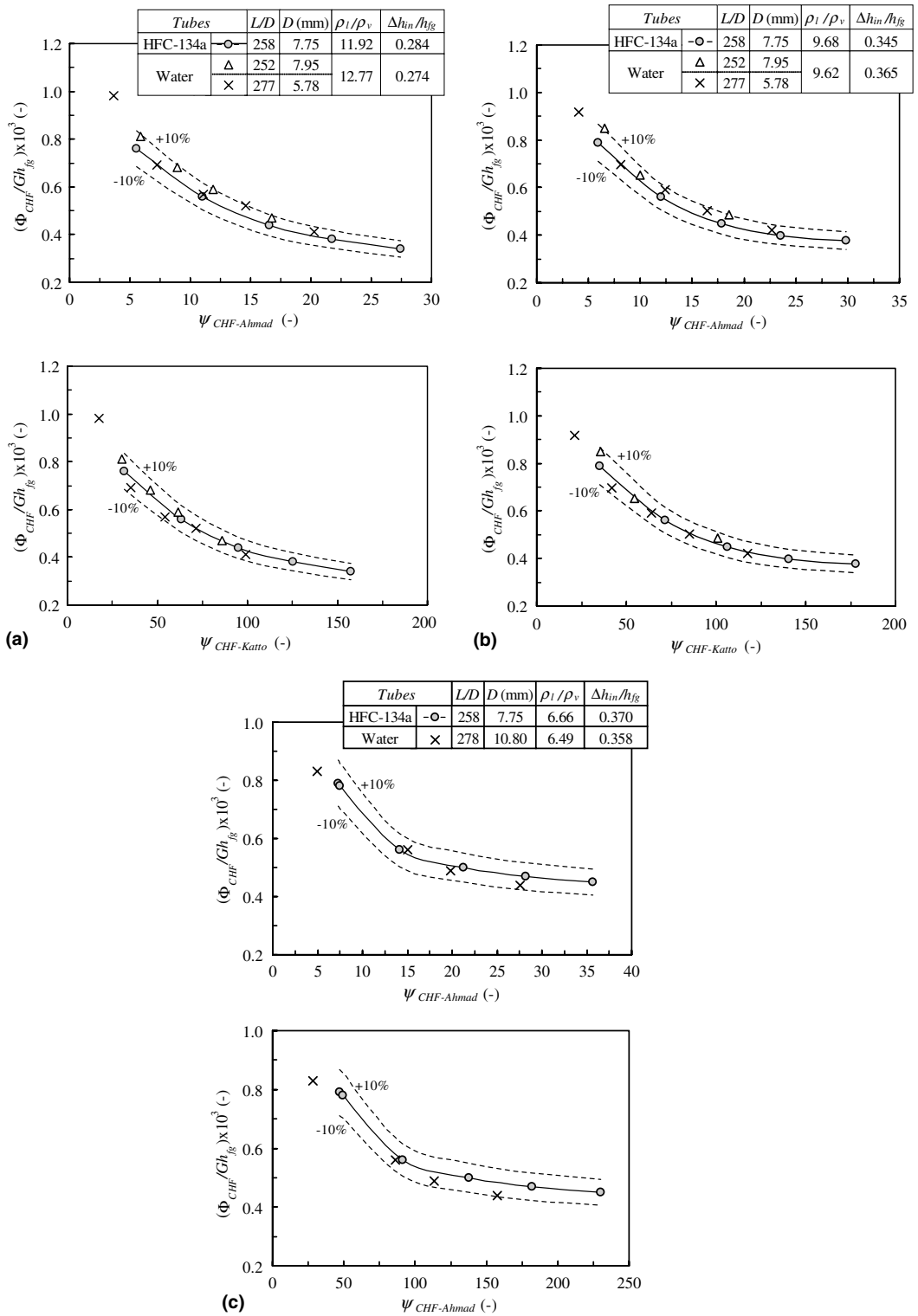

Fig. 6. (a) Comparison of the HFC-134a (at 1.70 MPa) and water (at 9.81 MPa) data in tubes, (b) comparison of the HFC-134a (at 1.96 MPa) and water (at 11.79 MPa) data in tubes and (c) comparison of the HFC-134a (at 2.48 MPa) and water (at 14.71 MPa) data in tubes.

Water CHF data in tubes used for the comparison with the HFC-134a CHF data are based on the KAIST (Korea Advanced Institute of Science and Technology) CHF data bank [15], which is based on 10822 CHF data for a stable upward flow of water in vertical round tubes. The similarity parameters $(L/D)_F$, $(\rho_l/\rho_v)_F$ and $(\Delta h_{in}/h_{fg})_F$ are calculated from the HFC-134a CHF experimental conditions. In the Freon fluid, a small pressure difference between the test section inlet and outlet leads to a large difference of the thermodynamic properties when compared with water. The inlet conditions, $\Delta h_{in}/h_{fg}$ are based on the inlet pressure conditions, and ρ_l/ρ_v, ψ_{CHF} and Φ_{CHF}/Gh_{fg} are based on the outlet pressure conditions. The water CHF data that agreed to within a deviation of ±8.0% with the values of the similarity parameters $(L/D)_F$, $(\rho_l/\rho_v)_F$ and $(\Delta h_{in}/h_{fg})_F$ for HFC-134a were selected.

Eqs. (4) and (7) show that if the similarity parameters L/D, ρ_l/ρ_v and $\Delta h_{in}/h_{fg}$ are the same for HFC-134a and water, both sets of the CHF data drawn on the plane of Φ_{CHF}/Gh_{fg} vs. ψ_{CHF} should be plotted on the same curve. For the comparison, the ranges of the flow parameters in the HFC-134a CHF data are the pressures from 1.70 to 2.48 MPa and the mass fluxes from 710 to 3500 kg m^{-2} s^{-1}, and in the water CHF data, the pressures are from 9.81 to 14.71 MPa and the mass fluxes are from 500 to 2900 kg m^{-2} s^{-1}. The inlet quality (i.e., $-\Delta h_{in}/h_{fg}$) and critical quality have ranges from −0.396 to −0.284 and from −0.02 to 0.48, respectively. Fig. 6(a)–(c) show the dimensionless CHFs for HFC-134a and water as a function of Ahmad's and Katto's modeling parameters for a mass flux with an error bound of ±10% for the HFC-134a data. In the present conditions, most of the data fall close to the same curve and as pointed out by Groeneveld et al. [8], the prediction errors for the dimensionless CHF by using the two modeling parameters of Eqs. (5) and (8) are approximately equal. Fig. 7 shows the comparison between the dimensionless CHFs with the Katto modeling parameter for L/D = 124–128 and 248–278 (L = 1.0–1.2 and 2.0–3.0 m, respectively). Two curves of the dimensionless CHF with the modeling parameter for both L/Ds have almost the same shape with a constant difference between each of the dimensionless CHF values. In addition, Figs. 6 and 7 show that there is scarcely an effect of the tube inner diameter, though D in the water data has a maximum deviation of ±39% from the HFC-134a data, when the geometric similarity L/D is maintained at a constant value (within a deviation of ±8.0% from D in the HFC-134a data).

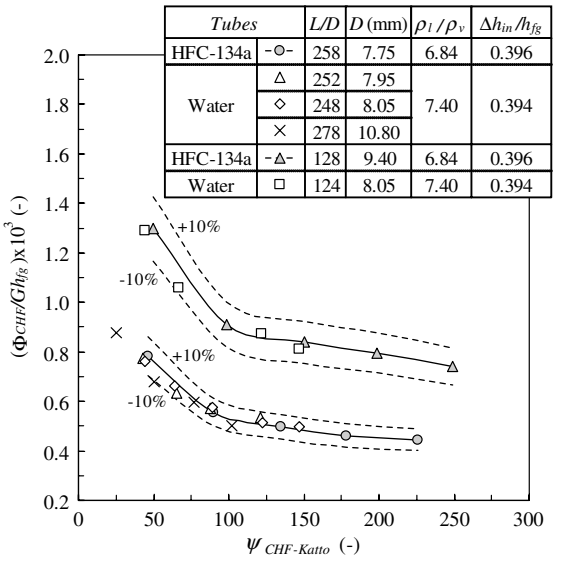

Fig. 7. Comparison of the HFC-134a and water data in tubes: effect of the geometric similarity parameter (L/D) on the dimensionless CHF.

4.2. Annulus

The typical results from the present HFC-134a experiments for an annulus are shown in Fig. 8, which shows the CHF as a function of the mass flux. The CHF increases monotonously as the mass flux increases. The slopes of the increasing CHF curves become gradual when the mass flux exceeds approximately 500 kg m^{-2} s^{-1}. The effect of an inlet subcooling on the CHF becomes small with the decreasing mass flux, and almost disappears at a mass flux of 150 kg m^{-2} s^{-1}. This behavior of the present CHF data agrees with the results of previous experimental studies [11,12], which were performed by using water as a working fluid in an annulus test section with the same geometry as the present experiments.

The water CHF data obtained in the previous experiments [11,12] are used for the comparison with the HFC-134a CHF data. Therefore, the geometric

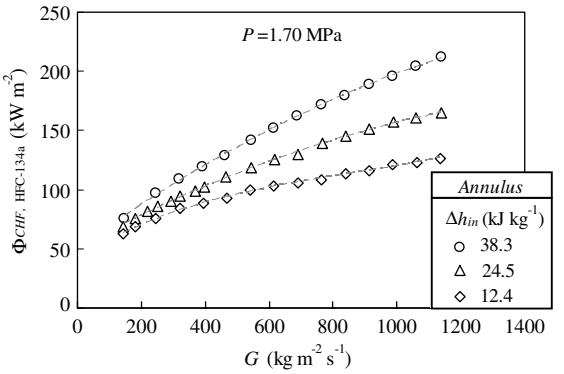

Fig. 8. HFC-134a CHF as a function of the mass flux in an annulus.

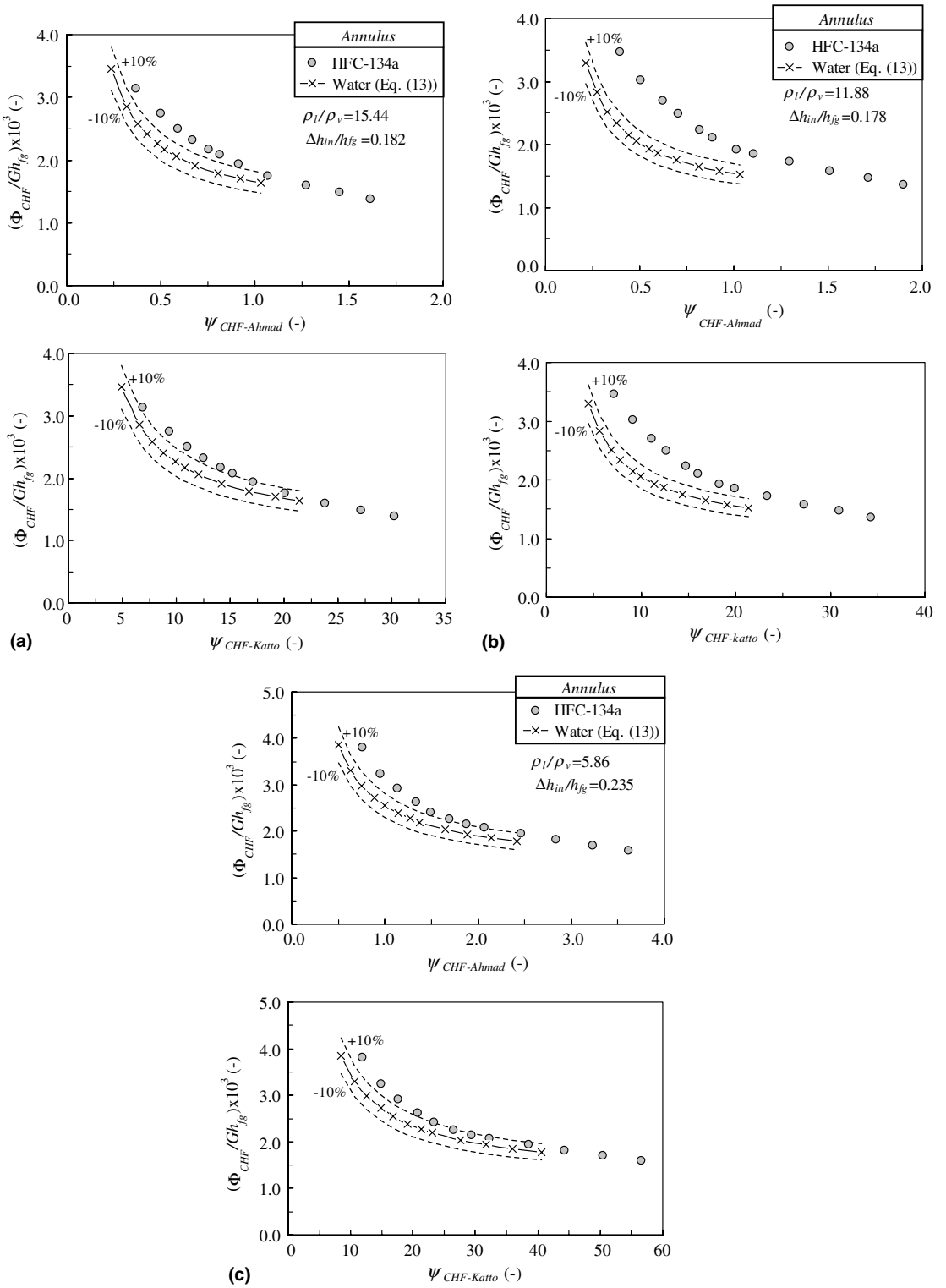

Fig. 9. (a) Comparison of the HFC-134a (at 1.40 MPa) and water (at 8.58 MPa) data in an annulus, (b) comparison of the HFC-134a (at 1.70 MPa) and water (at 10.30 MPa) data in an annulus and (c) comparison of the HFC-134a (at 2.66 MPa) and water (at 15.46 MPa) data in an annulus.

similarity is satisfied between the water and HFC-134a CHF data. However, the thermodynamic and hydrodynamic similarities were not maintained between both experiments because the experiments were carried out separately. Therefore, in the comparison of the annulus CHF data, the simple CHF correlation [16] which the authors developed based on the water CHF data is used. The correlation form is as follows:

$$\Phi_{\mathrm{CHF}} = [f(G,P) - g(P)Gx_{\mathrm{CHF}}](1 + C_7\Delta h_{\mathrm{in}}), \qquad (13)$$

where, $f(G,P) = (C_1 + C_2G + C_3P)$, $g(P) = (C_4 + C_5P + C_6P^2)$ and C_i are the fitting parameters (constants). This correlation predicts the water CHF with a uniform heat flux within a root mean square error of ±2.5% in the following conditions. The authors note that this correlation does not have any physical meaning.

- System pressure: 0.5–15.5 MPa (HFC-134a equivalent pressure: 0.1–2.7 MPa).
- Mass flux: 200–650 kg m^{-2} s^{-1}.
- Inlet subcooling: 85–350 kJ kg^{-1}.
- Critical quality: 0.11–0.54.

The above correlation includes the local parameter x_{CHF}. Therefore, the heat balance equation (11) is used to calculate the water CHF value. The pressure P, inlet subcooling h_{in} and latent heat h_{fg} in Eqs. (11) and (13) are determined by employing the similarities of Eqs. (2) and (3) from the HFC-134a CHF conditions. The mass flux conditions of the HFC134a experiments are substituted for G of Eq. (13). First by assuming a value of x_{CHF}, the CHFs are calculated with Eqs. (11) and (13), respectively, and these processes are then iterated until both the CHF values become equal.

The geometric similarity between the HFC-134a and water experiments in an annulus is satisfied with $L/D_{\mathrm{h}} = 186.5$. The effects of a gap and cold wall in an annular geometry do not need consideration for a comparison of both systems. The ranges of the flow parameters used for the comparison are pressures from 1.40 to 2.66 MPa for the HFC-134a CHF data (from 8.58 to 15.46 MPa in water equivalent) and mass fluxes from 150 to 690 kg m^{-2} s^{-1} for both CHF data. The inlet quality range is from −0.35 to −0.09. The water CHF correlation has an applicable range of inlet qualities of −0.36 to −0.04. The minimum and maximum data points of the modeling parameter ψ_{CHF} surpass the applicable range of the mass flux (200–650 kg m^{-2} s^{-1}) of the water CHF correlation. The critical qualities for some data points in the minimum mass fluxes (150 kg m^{-2} s^{-1}) for water exceed the maximum critical quality (0.54) available for the water CHF correlation. Therefore, the water dimensionless CHFs corresponding to the minimum and maximum values of the modeling parameters have some uncertainties.

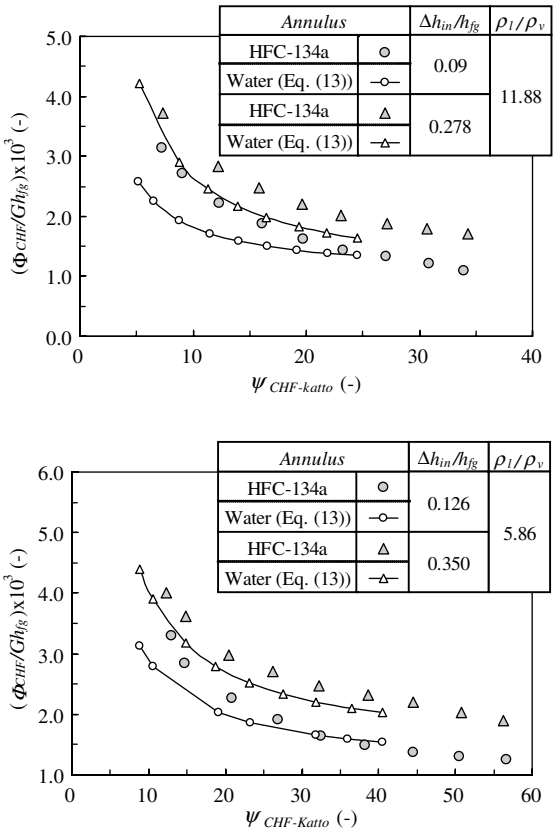

Fig. 10. Comparison of the HFC-134a and water data in an annulus: effect of the thermodynamic similarity parameter ($\Delta h_{\mathrm{in}}/h_{\mathrm{fg}}$) on the dimensionless CHF.

The comparison of the HFC-134a and water CHF data is shown as a function of Ahmad's and Katto's modeling parameters in Fig. 9(a)–(c). Since the dimensionless CHF values for water have some uncertainties, an error bound curve of ±10% is plotted for the water dimensionless CHFs in the figures. The data points show a large difference between the HFC-134a and the water CHF data. The water CHF data are considerably lower than the HFC-134a data. Especially, the difference is large at low values of the modeling parameters (i.e., low mass fluxes) and as the value of the modeling parameters increases, the water CHF curves approach the HFC-134a data points. The HFC-134a and the water CHF data curves may accord at a modeling parameter of about 30–40 (mass flux for the HFC-134a of about 600 kg m^{-2} s^{-1}). Fig. 9(a)–(c) show that the prediction errors for the dimensionless CHFs by using the Katto modeling parameter are slightly smaller when compared with the Ahmad modeling parameter. Fig. 10 shows the effect of the thermodynamic similarity parameter (i.e., the inlet quality) on the dimensionless CHFs, which are plotted as a function of Katto's modeling parameter. The dimensionless CHFs for the smaller values

($\Delta h_{in}/h_{fg} = 0.09$ and 0.126 in Fig. 10) of the thermodynamic similarity parameter show a large difference between the HFC-134a and the water in the low mass fluxes. For the large values (($\Delta h_{in}/h_{fg} = 0.278$ and 0.350) of the thermodynamic similarity parameter, the dimensionless CHF curves for water are fairly close to the HFC-134a data. This indicates that in the low mass flux and high quality conditions, the Katto and also the Ahmad modeling parameters cannot be correlated with the dimensionless CHF data for different fluids on the same curve.

5. Conclusions

The CHF experiments for HFC-134a as a working fluid have been performed for heated round tubes and an internally heated annulus with a uniform heat flux distribution. To provide the applicable range of the existing fluid-to-fluid modeling techniques, the HFC-134a and water CHF data have been compared by applying the Ahmad and the Katto modeling parameters. The following conclusions can be drawn from the present work:

1. In the tubes, the HFC-134a and water CHF data fall close to the same curve on the plane of the dimensionless CHF Φ_{CHF}/Gh_{fg} vs. the Ahmad and the Katto modeling parameters ψ_{CHF} in a range of mass fluxes from 710 to 3500 kg m^{-2} s^{-1} for HFC-134a.
2. In an annulus under low mass flux conditions, the dimensionless CHFs as a function of the Ahmad and the Katto modeling parameters show a large difference between the HFC-134a and the water. However, as the value of the modeling parameters, i.e., the mass flux, increases, the dimensionless CHF curves for water approach the HFC-134a data points.
3. The Katto and the Ahmad modeling parameters cannot be correlated with the dimensionless CHF data for HFC-134a and water on the same curve in the low mass flux and high quality conditions below about 600 kg m^{-2} s^{-1} for HFC-134a.

Acknowledgement

This study has been carried out under the Nuclear R&D Program supported by the Ministry of Science and Technology (MOST) of Korea.

References

[1] S.S. Doerffer, D.C. Groeneveld, R. Tain, S.C. Cheng, W. Zeggel, Fluid-to-fluid modeling of the critical heat flux in simple and complex geometries, Atomic Energy of Canada Limited, ARD-TD-321, 1991.

[2] R.M. Tain, S.C. Cheng, D.C. Groeneveld, Critical heat flux measurements in a round tube for CFCs and CFC alternatives, Int. J. Heat Mass Transfer 36 (1993) 2039–2049.

[3] R.M. Tain, D.C. Groeneveld, S.C. Cheng, Limitations of the fluid-to-fluid scaling technique for critical heat flux in flow boiling, Int. J. Heat Mass Transfer 38 (1995) 2195–2208.

[4] I.L. Pioro, D.C. Groeneveld, S.C. Cheng, S. Doerffer, A.Z. Vasic, Yu.V. Antoshko, Comparison of CHF measurements in R-134a cooled tubes and the water CHF look-up table, Int. J. Heat Mass Transfer 44 (2001) 73–88.

[5] I.L. Pioro, D.C. Groeneveld, L.K.H. Leung, S.S. Doerffer, S.C. Cheng, Yu.V. Antoshko, Y. Guo, A. Vasic, Comparison of CHF measurements in horizontal and vertical tubes cooled with R-134a, Int. J. Heat Mass Transfer 45 (2002) 4435–4450.

[6] G.F. Stevens, G.J. Kirby, A quantitative comparison between burn-out data for water at 1000 lb/in^2 and Freon-12 at 155 lb/in^2, uniformly heated round tubes, vertical upflow, United Kingdom Atomic Energy Authority, AEEW-R327, 1964.

[7] S.Y. Ahmad, Fluid to fluid modeling of critical heat flux: a compensated distortion model, Int. J. Heat Mass Transfer 16 (1973) 641–662.

[8] D.C. Groeneveld, B.P. Kiameh, S.C. Cheng, Prediction of critical heat flux (CHF) for non-aqueous fluids in forced convective boiling, in: Proceedings of the 8th International Heat Transfer Conference, San Francisco, USA, vol. 5, 1986, pp. 2209–2214.

[9] Y. Katto, A generalized correlation of critical heat flux for the forced convection boiling in vertical uniformly heated round tubes, Int. J. Heat Mass Transfer 21 (1978) 1527–1542.

[10] D.C. Groeneveld, S.C. Cheng, T. Doan, AECL-UO critical heat flux look-up table, Heat Transfer Eng. 7 (1–2) (1986) 46–62.

[11] S.Y. Chun, H.J. Chung, S.D. Hong, S.K. Yang, M.K. Chung, Critical heat flux in uniformly heated vertical annulus under a wide range of pressures −0.57 to 15.0 MPa, J. Korean Nucl. Soc. 32 (2) (2000) 128–141.

[12] S.Y. Chun, H.J. Chung, S.K. Moon, S.K. Yang, M.K. Chung, T. Schesse, M. Aritomi, Effect of pressure on critical heat flux in uniformly heated vertical annulus under low flow conditions, Nucl. Eng. Des. 203 (2001) 159–174.

[13] M.O. McLinden, S.A. Klein, E.W. Lemmon, A.P. Peskin, NIST REFPROP Database version 6.01/thermodynamic and transport properties of refrigerants and refrigerant mixtures, NIST Stand. Ref. database 23 (2003).

[14] ANSI/ASME PTC 19.1, ASME Performance Test Codes, Supplement on Instruments and Apparatus, Part 1, Measurement Uncertainty, Published by ASME, New York, 1985.

[15] S.H. Chang, W.P. Baek et al., The KAIST CHF data bank (Rev. 3), KAIST-NUSCOL-9601, 1996.

[16] S.K. Moon, S.Y. Chun, J.K. Park, W.P. Baek, Experimental study on the effect of axial heat flux on the CHF in low-flow conditions with vertical annuli, in: Proceedings of International Congress on Advances in Nuclear Power Plants (ICAPP '03), Cordoba, Spain, 2003, Paper No. 3289.